Appendix A

TERMS OF REFERENCE

for

Flood/Hydrology Specialist in connection with Khulekani Dam-break Study

The Flood/Hydrology Specialist will perform the following activities;

- carry out hydraulic analyses to establish the limits of the areas flooded at times of peak flow and the design capacity of the dam for flood control;
- carry out hydraulic analysis under different hypothesis of dam rupture to determine the water volumes, discharge rates, and arrival times of flood peaks;
- estimate areas flooded downstream of the dam for selected scenarios based upon activities 1 and 2 above;
- prepare a report on the findings of the consultancy.

The activities will be carried out based on existing information (drawings of the dam, maps of the downstream areas, etc).

Duty Station: Kathmandu

Duration: Two weeks (Kathmandu)

One week at home office for preparation and reporting

E.O.D.: September 1992

Language: English

El documento original no contiene las páginas 56

Appendix B
LIST OF REFERENCES

Feasibility report on Kulekhani Hydroelectric Project.
Japan International Cooperation Agency,
September 1974.

Tender Document (Specifications) for
Package A: Dam and Spillway,
Package B: Other Civil Works,
Volume II.
Nippon Koei Co., Ltd., Consulting Engineers,
July 1976.

Appraisal of the Kulekhani Hydroelectric Project,
International Bank for Reconstruction and Development (IBRD),
International Development Association (IDA)
March 15, 1975.

Kulekhani Hydroelectric Project,
Project Completion Report,
Nippon Koei Co., Ltd., Consulting Engineers,
October 1983.

Mission Report on Disaster Preparedness and Response in Nepal,
Royal Norwegian Ministry of Foreign Affairs/DHA
OCEANOR A/S
December 1990.

Midterm Evaluation Report of the Shivapuri Watershed Management and Fuelwood Plantation

Project,
FAO/Royal Norwegian Ministry of Foreign Affairs, 1987.

Hydrology Advisory Report for the Shivapuri Watershed Management and Fuelwood Plantation Project,
FAO
OCEANOR A/S, 1988.

Appendix C
ON THE BREACH MODEL

Breach: An Erosion Model for Earthen Dam Failures

by D. L. Fread[4]

July 1988

Abstract. A physically based mathematical model (BREACH) to predict the breach characteristics (size, time of formation) and the discharge hydrograph emanating from a breached earthen dam is presented. The earthen dam may be man-made or naturally formed by a landslide. The model is developed by coupling the conservation of mass of the reservoir inflow, spillway outflow, and breach outflow with the sediment transport capacity of the unsteady uniform flow along an erosion-formed breach channel. The bottom slope of the breach channel is assumed to be essentially that of the downstream face of the dam. The growth of the breach channel is dependent on the dam's material properties (D_{50} size, unit weight, friction angle, cohesive strength). The model considers the possible existence of the following complexities:

1) core material having properties which differ from those of the outer portions of the dam;
2) the necessity of forming an eroded ditch along the downstream face of the dam prior to the actual breach formation by the overtopping water;
3) the downstream face of the dam can have a grass cover or be composed of a material of larger grain size than the outer portion of the dam;
4) enlargement of the breach through the mechanism of one or more sudden structural collapses due to the hydrostatic pressure force exceeding the resisting shear and cohesive forces;
5) enlargement of the breach width by slope stability theory;
6) initiation of the breach via piping with subsequent progression to a free surface breach flow;
7) erosion transport can be for either noncohesive (granular) materials or cohesive (clay)

Senior Research Hydrologist with the Hydrologic Research Laboratory, National Weather Service, NOAA, Silver Springs, Maryland 20910

materials.

The outlfow hydrograph is obtained through a time-stepping iterative solution that requires only a few seconds for computation on a mainframe computer. The model is not subject to numerical stability or convergence difficulties. The model's predictions are compared with observations of a piping failure of the man-made Teton Dam in Idaho, the piping failure of the man-made Lawn Lake Dam in Colorado, and a breached landslide-formed dam in Peru. Also, the model has been used to predict possible downstream flooding from a potential breach of the landslide blockage of Spirit Lake in the aftermath of the eruption of Mount St. Helens in Washington. Model sensitivity to numerical parameters is minimal; however, it is sensitive to the internal friction angle of the dam's material and the extent of grass cover when simulating man-made dams and to the cohesive strength of the material composing landslide-formed dams.

Introduction

Earthen dams are subject to possible failure from either overtopping or piping water which erodes a trench (breach) through the dam. The breach formation is gradual with respect to time and its width as measured along the crest of the dam usually encompasses only a portion of the dam's crest length. In many instances, the bottom of the breach progressively erodes downward until it reaches the bottom of the dam; however, in some cases, it may cease its downward progression at some intermediate elevation between the top and bottom of the dam. The size of the breach, as constituted by its depth and its width (which may be a function of the depth), and the rate of the breach formation determine the magnitude and shape of the resulting breach outflow hydrograph. This is of vital interest to hydrologists and engineers concerned with real-time forecasting or evacuation planning for floods produced by dam failures.

This paper presents a mathematical model (BREACH) for predicting the breach characteristics (size, shape, time of formation) and the breach outflow hydrograph. The model is physically based on the principles of hydraulics, sediment transport, soil mechanics, the geometric and material properties of the dam, and the reservoir properties (storage volume,

spillway characteristics, and time dependent reservoir inflow rate). The dam may be either man-made or naturally formed as a consequence of a landslide. In either, the mechanics of breach formation are very similar, the principal difference being one of scale. The landslide-formed dam is often much larger than even the largest of man-made earthen dams as illustrated in Figure 1. The critical material properties of the dam are the internal friction angle, cohesive strength, and average grain size diameter (D_{50}).

The breach erosion model presented herein is a modification of an earlier version first reported by the author (Fread, 1984). The BREACH Model predicts a dam-breach outflow hydrograph. It differs from the parametric approach which the author has used in the NWS DAMBRK Model (Fread, 1977, 1981, 1983). The parametric model uses empirical observations of previous dam failures such as the breach width-depth relation, time of breach formation, and depth of breach to develop the outflow hydrograph. The breach erosion model presented herein can provide some advantages over the parametric breach model for application to man-made dams since the critical properties used by the model are measurable or can be estimated within a reasonable range from a qualitative description of the dam materials. However, it should be emphasized that even if the properties can be measured, there is a range for their probable value and within this range outflow hydrographs of varying magnitude and shape will be produced by the model. The hydrologist or engineer should investigate the most critical combination of values for the dam's material properties. It is considered essential when predicting breach outflows of landslide dams to utilize a physically based model since observations of such are essentially nonexistent, rendering the parametric approach infeasible.

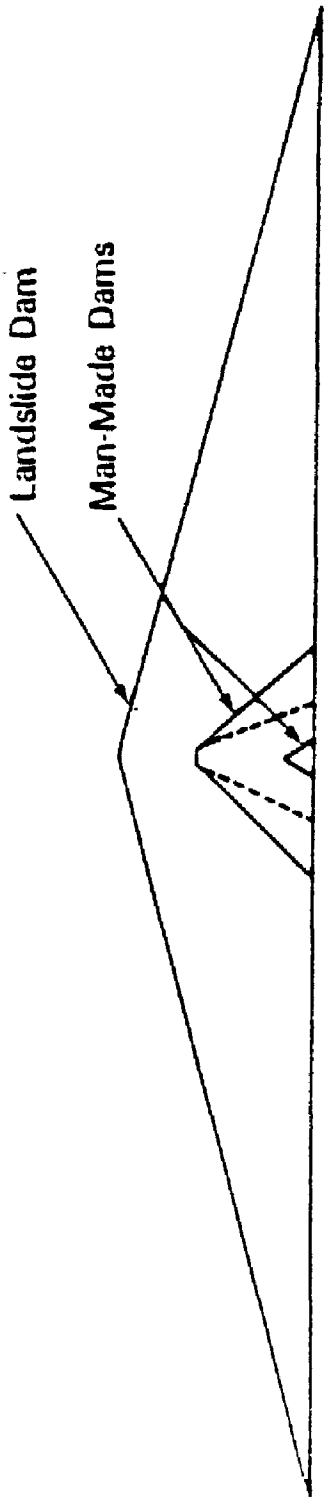

Figure 1: Comparative View of Natural Landslide Dams and Man-Made Dams

In this paper, the breach erosion model is applied to the piping initiated failures of the man-made Teton Dam in Idaho and the Lawn Lake Dam in Colorado; the overtopping failure of the Mantaro landslide-formed dam in Peru; and the possible failure of the landslide blockage of Spirit Lake near Mount St. Helens in Washington.

Previous Research

Other investigators of dam breach outflows have developed physically based models.

The first was Cristofano (1965) who derived an equation which related the force of the flowing water through the breach to the shear strength of the soil particles on the bottom of the breach and in this manner developed the rate of erosion of the breach channel as a function of the rate of change of water flowing through the breach. He assumed the breach bottom width to be constant with time and always of trapezoidal shape in which the side slopes of the trapezoid were determined by the angle of repose of the breach material, and the bottom slope of the breach channel was equal to the internal friction angle of the breach material. An arbitrary empirical coefficient which was critical to the model's prediction was also utilized.

Harris and Wagner (1967) used the Schoklitsch sediment transport equation and considered the breach to commence its downward progression immediately upon overtopping, and the erosion of the breach was assumed to progress to the bottom of the dam. Brown and Rogers (1977) presented a breach model which was based on the work of Harris and Wagner.

Most recently Ponce and Tsivoglou (1981) presented a rather computationally complex breach erosion model which coupled the Meyer-Peter and Muller sediment transport equation to the one-dimensional differential equations of unsteady flow and sediment conservation. Reservoir storage depletion was included in the upstream boundary equation used in conjunction with the unsteady flow equations. The set of differential equations was solved with a four-point implicit finite difference scheme. Flow resistance was represented through use of the Manning n. Breach width was empirically related to the rate of breach flow. A

small rivulet was assumed to be initially present along the flow path. "Outflow at start of the computation is a function of the assumed initial size of the rivulet. Progressive erosion widens and deepens the rivulet, increasing outflow and erosion rate in a self-generating manner. The upper cross-section on the sloping downstream face creeps upstream across the dam top until it reaches the upstream face, whereby rate of flow and erosion increase at a faster rate. If outflow increases enough to lower the reservoir level faster than the channel bed erodes, both outflow and erosion gradually diminish. Of course, outflow will eventually decrease even if the breach bed erodes all the way down to the stream bed. This mode of failure creates the outflow hydrograph in the shape of a sharp but nevertheless gradual flood wave." Ponce and Tsivoglou compared the model's predictions with observations of a breached landslide-formed dam on the Mantaro River in Peru. The results were considered good. However, they were influenced by the judicious selection of the Manning n, the breach width-flow relation parameter, and a coefficient in the sediment transport equation, although Ponce and Tsivoglou stated that the selected values were within each one's reasonable range of variation. Also, problems of a numerical computational nature were alluded to in connection with solving the implicit finite difference unsteady flow equations. They also implied that further work was needed to improve the breach width-flow relation and in developing a relation between the Manning n and the hydraulic/sediment characteristics of the breach channel.

The breach erosion model presented in this paper differs substantially from those previously reported. A summation of the important differences will be given after the model has been completely described in the next section.

Model Description

General

The breach erosion model (BREACH) simulates the failure of an earthen dam as shown in Figure 2. The dam may be homogeneous or it may consist of two materials: an outer zone with distinct material properties (ϕ - friction angle, C - cohesion, D_{50} - average grain size (mm), and Υ - unit weight), and an inner core with its ϕ, C, D_{50}, and Υ values. Also, the

downstream face of the dam may be specified as having: 1) a grass cover with specified length of either good or fair stand, 2) material identical to the outer portion of the dam, or 3) material of larger grain size than the outer portion. The geometry of the downstream face of the dam is described by specifying the top of the dam (H_u), the bottom elevation of the dam (H_l) or original streambed elevation, and its slope as given by the ratio 1 (vertical) : ZD (horizontal). Then, the geometry of the upstream face of the dam is described by specifying its slope as the ratio 1 (vertical) : ZU (horizontal). If the dam is man-made it is further described by specifying a flat crest width (W_{cr}) and a spillway rating table of spillway flow vs. head on the spillway crest. Naturally formed landslide dams are assumed to not have a flat crest or, of course, a spillway.

The storage characteristics of the reservoir are described by specifying a table of surface area (S_a) in units of acre-ft vs. water elevation, the initial water surface elevation (H_i) at the beginning of the simulation, and a table of reservoir inflows (Q_i) in cfs vs. the hour of their occurrence (T_i).

If an overtopping failure is simulated, the water level (H) in the reservoir must exceed the top of the dam before any erosion occurs. The first stages of the erosion are only along the downstream face of the dam as denoted by the line A-A in Figure 2 where, initially if no grass cover exists, a small rectangular-shaped rivulet is assumed to exist along the face. An erosion channel of depth-dependent width is gradually cut into the downstream face of the dam. The flow into the channel is determined by the broad-crested weir relationship:

$$Q_b = 3\ B_0\ (H\text{-}H_c)^{1.5}$$

in which Q_b is the flow into the breach channel, B_0 is the instantaneous width of the initially rectangular-shaped channel, and H_c is the elevation of the breach bottom. As the breach erodes into the downstream face of the dam, the breach bottom elevation (H_c) remains at the top of the dam (H_u), and the most upstream point of the breach channel moves across the crest of the dam towards the dam's upstream face. When the bottom of the erosion channel has attained the position of line B-B in Figure 2, the breach bottom (H_c) starts to erode vertically downward. The breach bottom is allowed to progress downward until it reaches the bottom elevation of the dam H_l.

If the downstream face of the dam (line A-A in Figure 2) has a grass cover, the velocity of the overtopping flow along the grassed downstream face is computed at each time step by the Manning equation. This velocity is compared with a specified maximum permissible velocity for grass-lined channels (see Chow, 1959). Failure of the downstream face via erosion is initiated at the time when the permissible velocity is exceeded. At that time a single rivulet having dimensions of one (ft) depth x two width is instantly created along the downstream face. Erosion within the rivulet is allowed to proceed as in the case where a grass cover does not exist. The velocity (v) along the downstream face is computed as follows:

$$q = 3\ (H-H_c)^{1.5} \tag{2}$$

$$y = \left[\frac{qn'}{1.49\ (1/ZD)^{0.5}}\right]^{0.6} \tag{3}$$

$$n' = aq^b \tag{4}$$

$$v = q/y \tag{5}$$

in which q is the overtopping flow per foot of crest length, $(H-H_c)$ is the hydrostatic head (ft) over the crest, n' is the Manning coefficient for grass-lined channels (Chow, 1959), a and b are fitting coefficients required to represent in mathematical form the graphical curves given in Chow.

If a piping breach is simulated, the water level (H) in the reservoir must be greater than the assumed center-line elevation (H_p) of the initially rectangular-shaped piping channel before the size of the pipe starts to increase via erosion. The bottom of the pipe is eroded vertically downward while its top erodes at the same rate vertically upwards. The flow into the pipe is controlled by orifice flow, i.e.,

$$Q_b = A\ [2g\ (H-H_p) / (1 + fL/D)]^{0.5} \tag{6}$$

in which Q_b is the flow (cfs) through the pipe, g is the gravity acceleration constant, A is the cross-sectional area (ft^2) of the pipe channel, $(H-H_p)$ is the hydrostatic head (ft) on the pipe,

L is the length (ft) of the pipe channel, D is the diameter or width (ft) of the pipe, and f is the Darcy friction factor computed from the following mathematical representation of the Moody curves (Morris and Wiggert, 1972):

$$f = 64/N_R \quad \ldots\ldots\ldots\ldots\ldots\ldots \quad N_R < 2000 \tag{7}$$

$$f = 0.105 \left(\frac{D_{50}}{D}\right)^{0.167} \quad \ldots\ldots\ldots\ldots \quad N_R \geq 2000 \tag{8}$$

$$N_R = 83333\ Q_b\ D/A \tag{9}$$

in which f is the Darcy friction factor and N_R is the Reynolds number. As the top elevation (H_{pu}) of the pipe erodes vertically upward, a point is reached when the flow changes from orifice-control to weir-control when the head on the pipe is less than the pipe diameter. The transition is assumed to occur when the following inequality is satisfied:

$$H < H_p + 2\ (H_{pu} - H_p) \tag{10}$$

The weir flow is then governed by Eq. (1) in which H_c is equivalent to the bottom elevation of the pipe and B_0 is the width of the pipe at the instant of transition. Upon reaching the instant of flow transition from orifice to weir, the remaining material above the top of the pipe and below the top of the dam is assumed to collapse and is transported along the breach channel at the current rate of sediment transport before further erosion occurs. The erosion then proceeds to cut a channel parallel to and along the remaining portion of the downstream face of the dam between the elevation of the bottom of the pipe and the bottom of the dam. The remaining erosion process is quite similar to that described for the overtopping type of failure with the breach channel now in a position similar to line A-A in Figure 2.

The preceding general description of the erosion process was for a man-made dam. If a landslide dam is simulated the process is identical except, due to the assumption that the landslide dam has no crest width (W_{cr}), the erosion initially commences with the breach channel in the position of line B-B in Figure 2. A failure mode of overtopping or piping may be initiated for a landslide-formed dam.

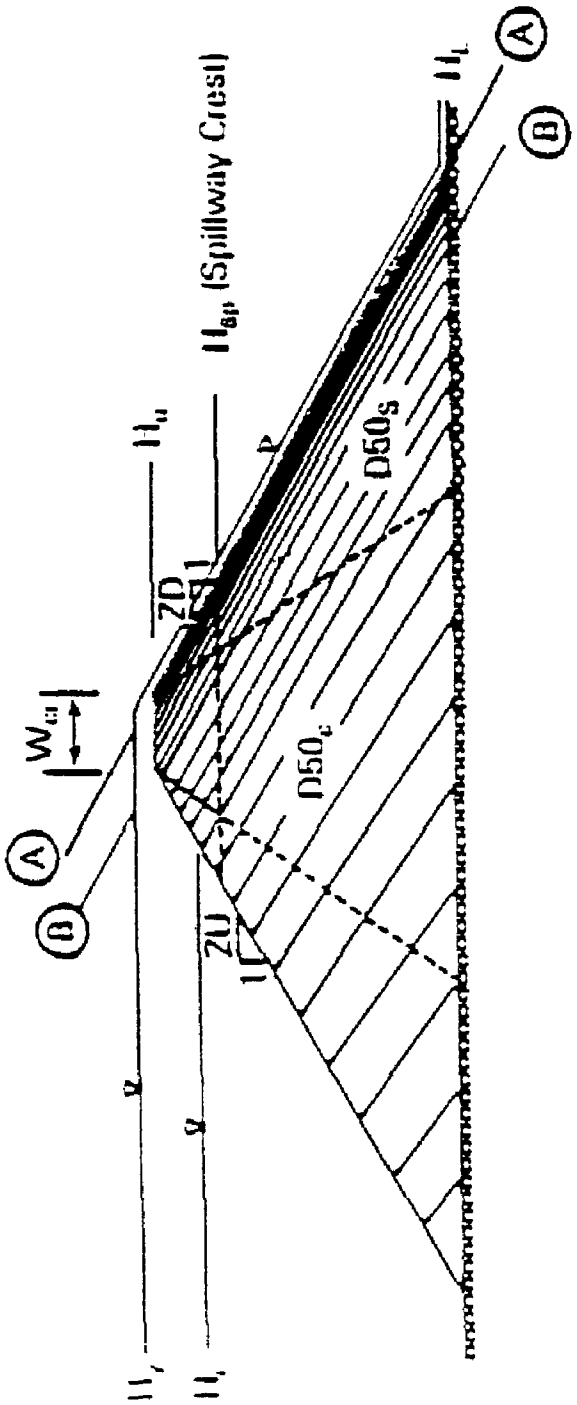

Figure 2: Front View of Dam Width Breach Formation Sequence

Breach Width

The method of determining the width of the breach channel is a critical component of any breach model. In this model the width of the breach is dynamically controlled by two mechanisms. The first assumes the breach has an initial rectangular shape as shown in Figure 3. The width of the breach (B_0) is governed by the following relation:

$$B_0 = B_r\, y \tag{11}$$

in which B_r is a factor based on optimum channel hydraulic efficiency and y is the depth of flow in the breach channel. The parameter B_r has a value of 2 for overtopping failures while for piping failures, B_r is set to 1.0. The model assumes that y is the critical depth at the entrance to the breach channel, i.e.,

$$y = 2/3\ (H-H_c). \tag{12}$$

The second mechanism controlling the breach width is derived from the stability of soil slopes (Spangler, 1951). The initial rectangular-shaped channel changes to a trapezoidal channel when the sides of the breach channel collapse, forming an angle (α) with the vertical. The collapse occurs when the depth of the breach cut (H_c') reaches the critical depth (H') which is a function of the dam's material properties of internal friction (ϕ), cohesion (C), and unit weight (Υ), i.e.

$$H_k' = \frac{4\, C \cos\phi \sin\theta_{k-1}'}{\Upsilon\,[\,1-\cos(\theta_{k-1}'-\phi)\,]} \quad \ldots\ldots\ldots \quad k = 1,2,3 \tag{13}$$

in which the subscript k denotes one of three successive collapse conditions as shown in Figure 3, and θ is the angle that the side of the breach channel makes with the horizontal as shown in Figure 4. Thus, the angle (θ) or (α) at any time during the breach formation is given as follows:

$$\theta = \theta_{k-1}' \quad \ldots\ldots\ldots\ldots\ldots\ldots \quad H_k \le H_k' \tag{14}$$

$$\theta = \theta_k' \quad \ldots\ldots\ldots\ldots\ldots\ldots \quad H_k > H_k' \tag{15}$$

$$B_0 = B_r\, y \quad \ldots\ldots\ldots\ldots\ldots\ldots \quad k = 1 \tag{16}$$

$$B_0 = B_{om} \quad \ldots\ldots\ldots\ldots\ldots\ldots \quad k > 1 \tag{17}$$

$$B_{om} = B_r\, y \quad \ldots\ldots\ldots\ldots\ldots\ldots \quad \text{when } H_1 = H_1' \tag{18}$$

$$\alpha = 0.5\,\pi - \theta \tag{19}$$

where:

$$\theta_0' = 0.5\,\pi \tag{20}$$

$$\theta_k' = (\theta_{k-1}' + \phi) / 2 \quad \ldots\ldots\ldots\ldots \quad k = 1,2,3 \tag{21}$$

$$H_k = H_c' - y/3 \tag{22}$$

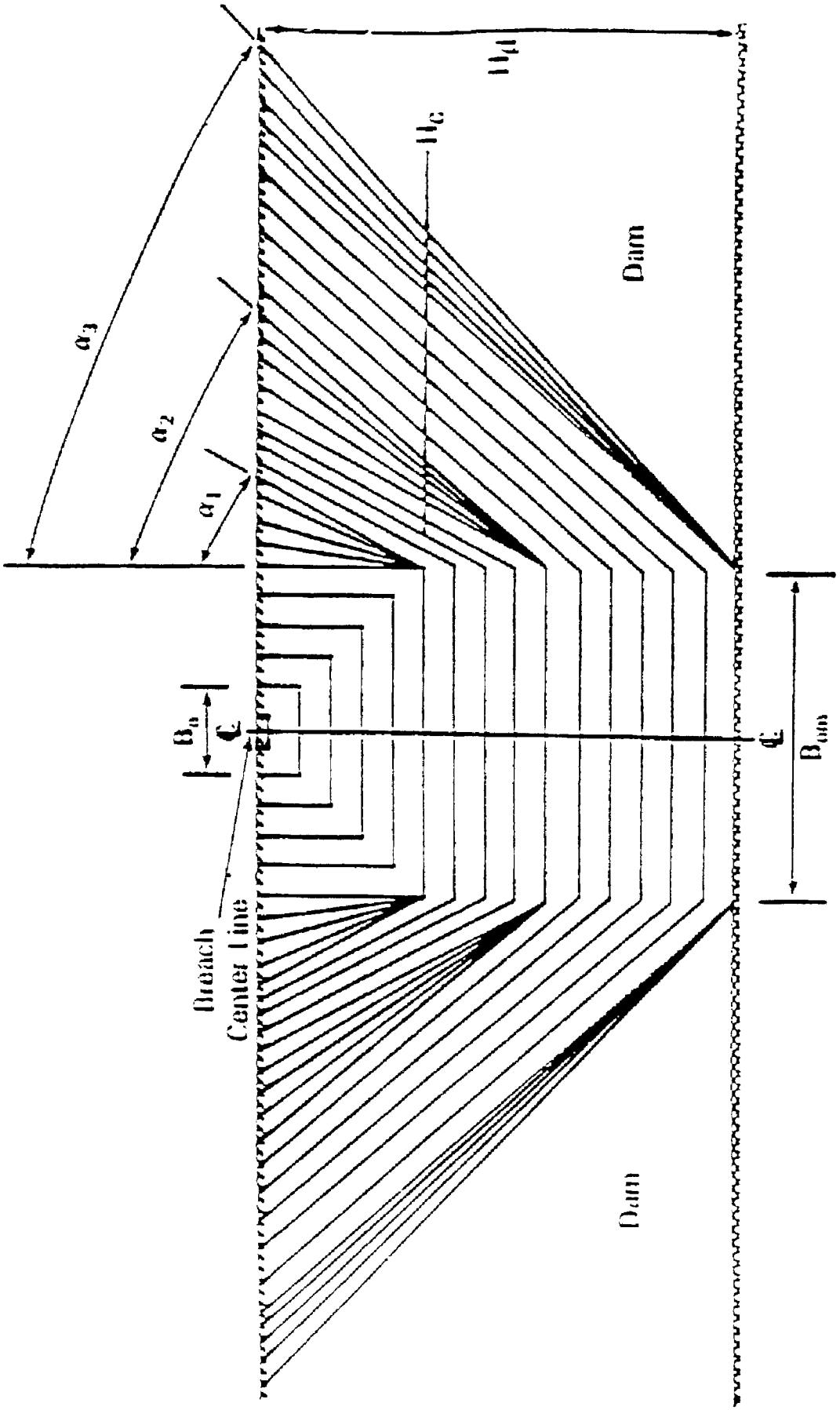

Figure 3: Front View of Dam with Breach Formation Sequence

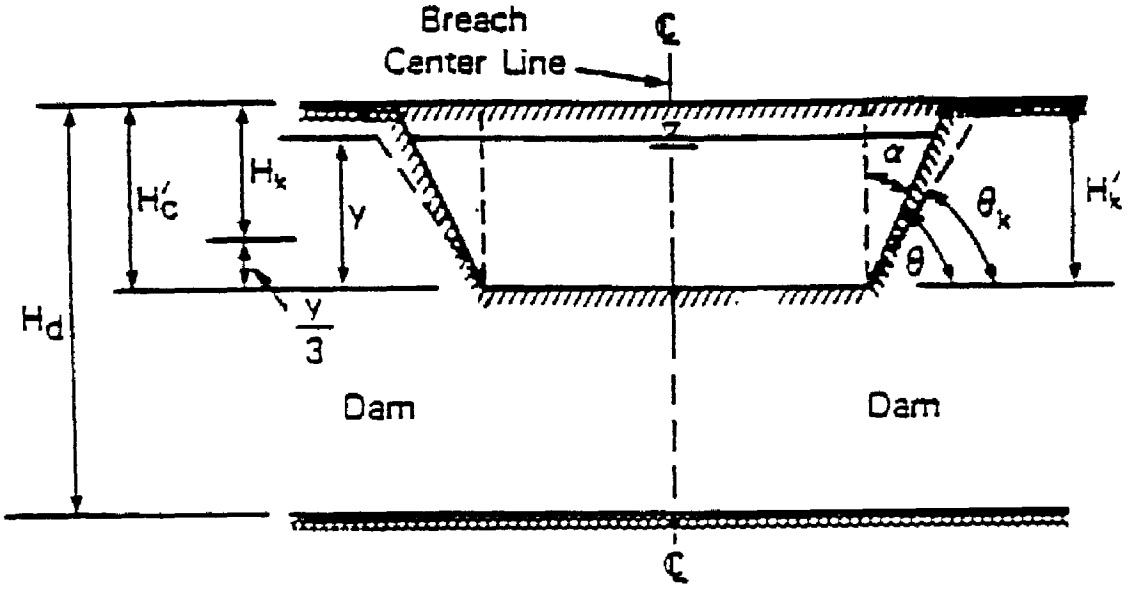

Figure 4: Front View of Dam with Breach

The subscript (k) is incremented by 1 at the instant when $H_k > H_k'$. In Eq. (22), the term (y/3) is subtracted from H_c' to give the actual free-standing depth of breach cut in which the supporting influence of the water on the stability of the sides of the breach is taken into account. Through this mechanism, it is possible for the breach to widen after the peak outflow through the breach has occurred since the flow depth (y) diminishes during the receding flow.

Erosion is assumed to occur equally along the bottom and sides of the breach channel except when the sides of the breach channel collapse. Thereupon the breach bottom is assumed not to continue to erode downward until the volume of collapsed material along the breach is removed at the rate of the sediment transport capacity of the breach channel at the instant of collapse. After this characteristically short pause, the breach bottom and sides continue to erode.

When the breach has eroded downward to the original valley floor, further downward erosion is prohibited within the model; however, the sides of the breach continue to erode and the breach continues to widen. The occurrence of the outflow peak discharge may coincide with the breach bottom reaching the valley floor or at some time later as the breach sides continue to be eroded. The maximum discharge through the breach is dependent on the rate of breach enlargement via erosion and the rate at which the reservoir head decreases as a result of the increasing flow caused by the increasing breach opening. The model allows a maximum permissible breach bottom width and a maximum top width at the crest of the dam to be specified by the user; this approximately accounts for the original valley topography which is assumed to be nonerodible.

When landslide dams are simulated, the relatively long breach channel lengths, compared to those of man-made dams, suggest that the width for the channel be computed apart from the entrance width of the breach. In this case, y in Eqs. (11), (16), (18), and (22) is computed as the normal uniform depth (y_n) in the breach channel rather than the critical depth given by Eq. (12). Equations for computing the normal channel depth are presented in a subsequent section.

Reservoir Level Determination

$$\overline{Q_i} - (\overline{Q_b} + \overline{Q_{sp}} + \overline{Q_0}) = S_a \frac{\Delta H \, 43560}{\Delta t \, 3600} \quad (23)$$

in which ΔH is the change in water surface elevation during the time interval (Δt), and S_a is the surface area in acres at elevation H. All flows are expressed in units of cfs and the bar (-) indicates the flow is averaged over the time step. Rearranging Eq. (23) yields the following expression for the change in the reservoir water surface:

$$\Delta H = \frac{0.0826 \, \Delta t}{S_a} \quad (\overline{Q_i} - \overline{Q_b} - \overline{Q_{sp}} - \overline{Q_0}) \quad (24)$$

The reservoir elevation (H) at time (t) can easily be obtained from the relation,

$$H = H' + \Delta H \quad (25)$$

in which H' is the reservoir elevation at time $t - \Delta t$.

The reservoir inflow ($\overline{Q_i}$) is determined from the specified table of inflows (Q_i) vs. time (T_i). The spillway flow ($\overline{Q_s}$) is determined from the specified table of spillway flows (Q_s) vs. reservoir elevation (H). The breach flow (Q_b) is computed from Eq. (2) for piping flow. When the breach flow is weir-type, Eq. (1) is used when $H_c = H_u$; however, when $H_c < H_u$, the following broad-crested weir equation is used:

$$Q_b = 3 \, B_0 \, (H - H_c)^{1.5} + 2 \tan (\alpha) \quad (H - H_c)^{2.5} \quad (26)$$

in which B_0 is given by Eq. (16) or Eq. (17) and α is given by Eq. (19). The crest overflow is computed as broad-crested weir flow from Eq. (1), where B_0 is replaced by the crest length of the dam and H_c is replaced by H_u.

Breach Channel Hydraulics

The breach flow is assumed to be adequately described by quasi-steady uniform flow

as determined by applying the Manning open channel flow equation at each Δ t time step, i.e.,

$$Q_b = \frac{1.49}{n} S^{0.5} \frac{A^{1.67}}{p^{0.67}} \quad (27)$$

in which S = 1 /ZD, A is the channel cross-sectional area, P is the wetted perimeter of the channel, and n is the Manning coefficient. In this model, n is computed using the Strickler relation which is based on the average grain size of the material forming the breach channel, i.e.,

$$n = 0.013\ D_{500}^{\ 0.167} \quad (28)$$

in which D_{50} represents the average grain size diameter expressed in mm.

The use of quasi-steady uniform flow is considered appropriate because the extremely short reach of breach channel, very steep channel slopes (1/ZD) for man-made dams, and even in the case of landslide dams where the channel length is greater and the slope is smaller, contribute to produce extremely small variation in flow with distance along the breach channel. The use of quasi-steady uniform flow in contrast to the unsteady flow equations as used by Ponce and Tsivoglou (1981) greatly simplifies the hydraulics and computational algorithm. Such simplification is considered commensurate with the other simplifications inherent in the treatment of the breach development in dams for which precise measurements of material properties are lacking or impossible to obtain and the wide variance which exists in such properties in many dams. The simplified hydraulics eliminates troublesome numerical computation problems and enables the breach model to require only minimal computational resources.

When the breach channel is rectangular, the following relations exist between depth of flow (y_n) and discharge (Q_b):

$$Y_n = \left(\frac{Q_b\, n}{1.49\, B_0\, S^{0.5}} \right) 0.6 \tag{29}$$

in which B_0 is defined by Eqs. (16-18).

When the breach channel is trapezoidal, the following algorithm based on Newton-Raphson iteration is used to compute the depth of low (y_n):

$$y_n^{\,k+1} = y_n^{\,k} - \frac{f(y_n^{\,k})}{f'(y_n^{\,k})} \tag{30}$$

$$f(y_n^{\,k}) = Q_b\, P^{0.67} - 1.49\; S^{0.5}\; A^{1.67} \tag{31}$$

in which

$$A = 0.5\,(B_0 + B)\, y_n^{\,k} \tag{32}$$

$$B = B_{om} + y_n \tan(\alpha) \tag{33}$$

$$P = B_{om} + y_n / \cos(\alpha) \tag{34}$$

$$f'(y_n^{\,k}) = 0.67\, Q_b \frac{P'}{P^{1/3}} - 1.67\, \frac{1.49}{n}\, S^{0.5}\; B\; A^{0.67} \tag{35}$$

in which

$$P' = 1/\cos(\alpha). \tag{36}$$

The superscript (k) is an iteration counter; the iteration continues until

$$| y_n^{k+1} - y_n^{k} | < \varepsilon \qquad \varepsilon \leq 0.01 \tag{37}$$

The first estimate for y_n is obtained from the following:

$$y_n^{1} = \left(\frac{Q_b n}{1.49\ B\ S^{0.5}} \right) 0.6 \tag{38}$$

where:

$$\overline{B} = 0.5\ (B_{om} + B\ ') \tag{39}$$

in which B ' is the breach channel top width at the water depth (y_n) at (t -t Δ).

Sediment Transport

The rate at which the breach is eroded depends on the capacity of the flowing water to transport the eroded material. The Meyer-Peter and Muller sediment transport relation as modified by Smart (1984) for steep channels is used, i.e.,

$$Q_s = 3.64\ (D_{90} / D_{30})^{0.2}\ P\ \frac{D^{2/3}}{n}\ S^{1.1}\ (DS - T) \tag{40}$$

where:

$$T = 0.0054\ \tau_c = D_{50} \qquad \text{(noncohesive)} \tag{41}$$

$$T = \frac{h'}{62.4}\ (PI)^{C'} \qquad \text{(cohesive)} \tag{42}$$

$$\tau_c = a'\ \tau'_c \tag{43}$$

$$a' = \cos\theta\ (1.0 - 1.54 \tan\theta) \tag{44}$$

$$\theta = \tan^{-1} S \tag{45}$$

$$\tau_c^* = 0.122 / R^{*0.970} \quad \ldots\ldots\ldots \quad R^* < 3 \tag{46}$$

$$\tau_c^* = 0.056 / R^{*0.266} \quad \ldots\ldots\ldots \quad 3 \leq R^* \leq 10 \tag{47}$$

$$\tau_c^* = 0.0205\, R^{*0.173} \quad \ldots\ldots\ldots \quad R^* > 10 \tag{48}$$

$$S = \frac{1}{ZD} \tag{49}$$

$$R^* = 1524\, D_{50}\, (DS)^{0.5} \tag{50}$$

in which Q_s is the sediment transport rate (cfs); D_{30}, D_{50}, D_{00} (mm) are grain sizes at which 30, 50, and 90 percent of the total weight is finer; D is the hydraulic depth of flow (ft), S is the slope of the downstream face of the dam; and τ_c^* is the Shields' dimensionless critical shear stress, PI is the plasticity index for cohesive soils, b' and c' are empirical coefficients with the following ranges: $0.002 \leq b' \leq 0.019$ and $0.54 \leq c' \leq 0.84$, respectively (Clapper and Chen, 1987).

Breach Enlargement By Sudden Collapse

It is possible for the breach to be enlarged by a rather sudden collapse failure of the upper portions of dam in the vicinity of the breach development. Such a collapse would consist of a wedge-shaped portion of the dam having a vertical dimension (Y_c) as shown in Figure 5. The collapse would be due to the pressure of the water on the upstream face of the dam exceeding the resistive forces due to shear and cohesion which keep the wedge in place. When this occurs, the wedge is pushed to the right in Figure 6 and is then transported by the escaping water through the now enlarged breach. When collapse occurs, the erosion of the breach ceases until the volume of the collapsed wedge is transported through the breach channel at the transport rate of the water escaping through the breach channel at the transport rate of the water escaping through the suddenly enlarged breach. A check for collapse is made at each Δt time step during the simulation. The collapse check consists of assuming

an initial value for Y_c of 10 and then summing the forces acting on the wedge of height, Y_c. The forces are those due to the water pressure (F_w) and the resisting forces which are the shear force (F_{sb}) acting along the bottom of the wedge, the shear force (F_{ss}) acting along both sides of the wedge, the force (F_{cb}) due to cohesion along the wedge bottom and (F_{cs}), the force due to cohesion acting along the sides of the wedge. Thus, collapse occurs if:

$$F_w > F_{sb} + F_{ss} + F_{cb} + F_{cs} \tag{51}$$

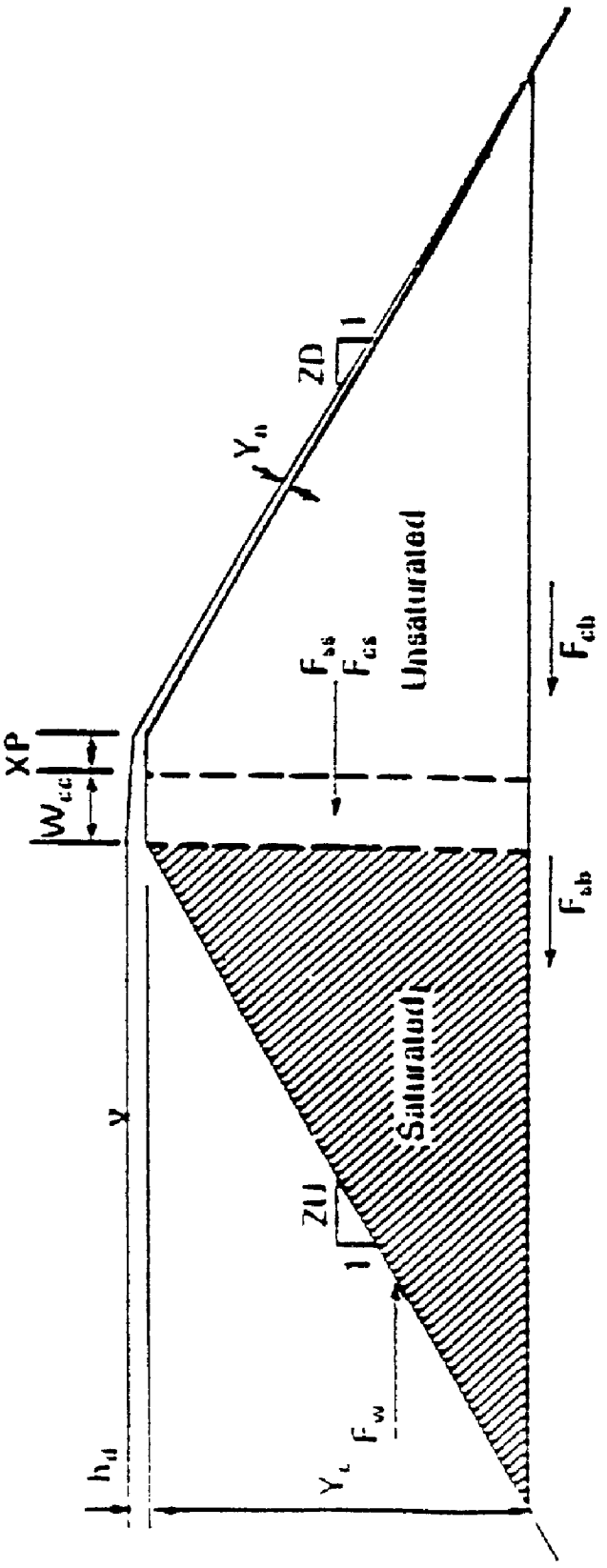

Figure 5: Side View of Dam Showing the Forces which Determine the Possible Collapse of the Upper Portion (Y_c) of the Dam

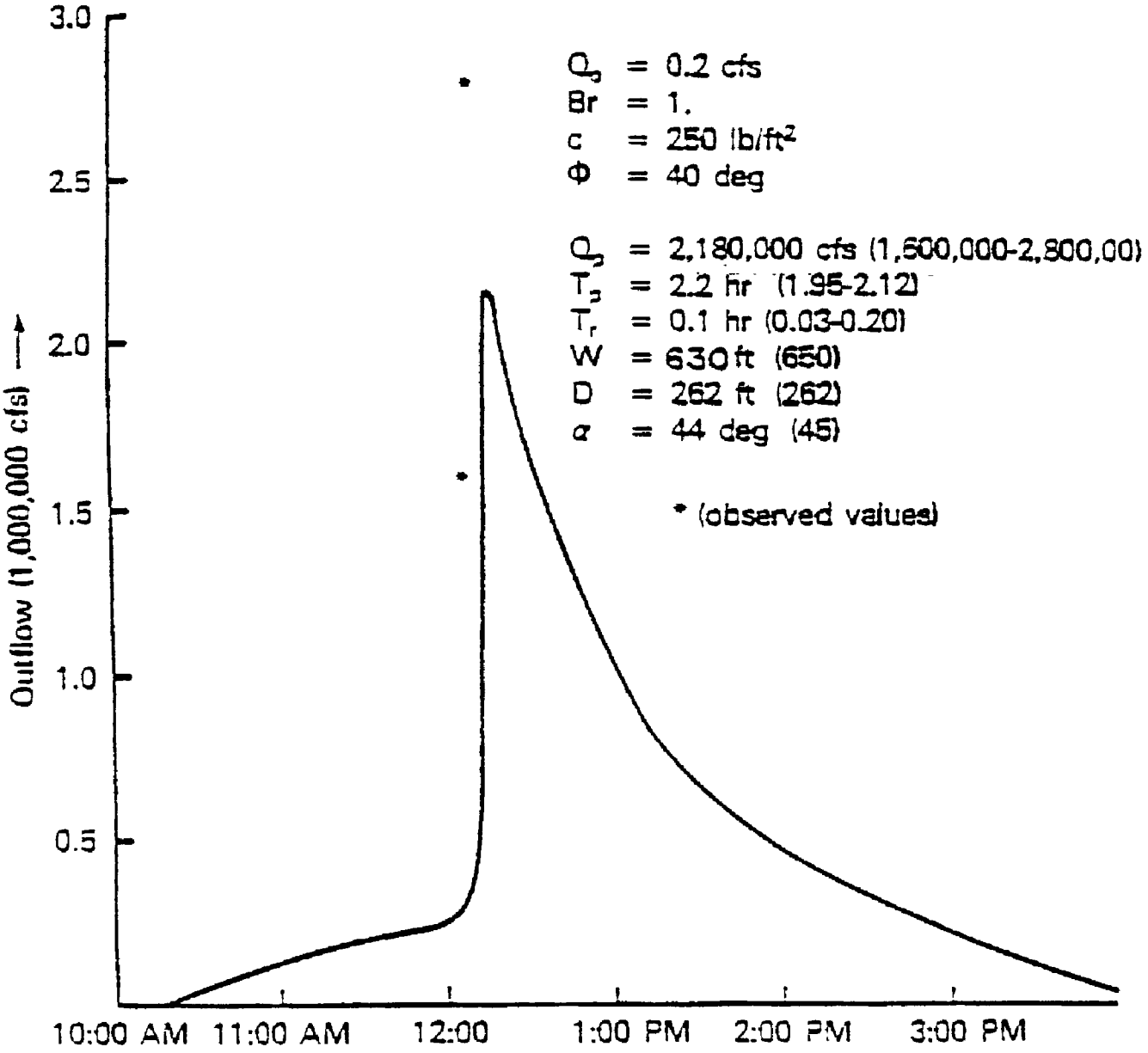

Figure 6: Teton Dam: Predicted and Observed Breach Outflow Hydrograph and Breach Properties

where:

$$F_w = 0.5 \; 62.4 \; \overline{B} \; (Y_c + 2 \; h_d) \tag{52}$$

$$F_{sb} = \tan\theta \; [\; (\Upsilon - 62.4) \; 0.5 \; ZU \; B \; Y_c^2 + \Upsilon \; B \; W_{cc} \; Y_c + \Upsilon \; 0.5 \; ZD \; \overline{B} \; Y_c^2 + 0.67 \; 62.4 \; h_d \; W_{cc} \; B + 62.4 \; ZD' \; B \; y_n \; Y_c \;] \tag{53}$$

$$F_{ss} = \Upsilon K \tan\phi \; Y_c^2 \; [\; W_{cc} + (ZU + ZD) \; Y_c \;] \tag{54}$$

$$F_{cb} = C B_0 \; [\; W_{cc} + (ZU + ZD) \; Y_c \;] \tag{55}$$

$$F_{cs} = 2C \; [\; W_{cc} + (ZU + ZD) \; Y_c \; (\; B_0 + 2Y_c / \cos\alpha) \;] \tag{56}$$

in which

$$K = (\; 1 - \sin\phi \;) / (\; 1 + \sin\phi \;) \tag{57}$$

$$\overline{B} = B_0 + H_c \sin\alpha \tag{58}$$

$$ZD' = (\; 1 + ZD^2 \;)^{0.5} \tag{59}$$

and Y_c , h_d , ZU, W_{cc} , and y_n are defined in Figure 5. The top width (B) of the water surface in the breach channel is defined by Eq. (11) or Eq. (33), and α is defined in Figure 4 and Eq. (19).

If the inequality of Eq. (51) is not satisfied with the first trail Y_c , then no collapse occurs at this time. If it is satisfied, Y_c is increased by 2 ft and Eq. (51) is again evaluated. This cycle continues until the inequality is not satisfied. Then the final value for Y_c is assumed to be Y_c-1.

Computational Algorithm

The sequence of computations in the model are iterative since the flow into the breach

is dependent on the bottom elevation of the breach and its width while the breach properties are dependent on the sediment transport capacity of the breach flow, and the transport capacity is dependent on the breach size and flow. A simple iterative algorithm is used to account for the mutual dependence of the flow, erosion, and breach properties. An estimated incremental erosion depth ($\Delta H_c'$) is used at each time step to start the iterative computation. This estimated value can be extrapolated from previously computed incremental erosion depths after the first few time steps. The computational algorithm follows:

1. increment the time: $t = t' + \Delta t$;
2. compute H_c using estimated $\Delta H_c'$: $H_c = H_c' - \Delta H_c'$;
3. compute reservoir elevation: $H = H' + \Delta H$, where $\Delta H'$ is an estimated incremental change in the reservoir elevation as obtained by extrapolation from previous changes and H' is the reservoir elevation at time (t') ;
4. compute $\overline{Q_{sp}}$, $\overline{Q_t}$, $\overline{Q_0}$ associated with elevation H ;
5. compute ΔH from Eq. (24) using the previously computed breach flow (Q_b);
6. compute reservoir elevation: $H = H' + \Delta H$;
7. compute breach flow (Q_b) using Eq. (1), Eq. (2), or Eq. (26);
8. correct breach flow for downstream submergence:

   $Q_b = S_b Q_b$, where $Sb = 1.0 - \left(\frac{Y_t - H_c}{H - H_c}\right) - 0.67)^3$

   in which y_t is the tailwater depth due to the total outflow ($Q_b + Q_{sp} + Q_0$), and is computed from the Manning equation applied to the tailwater cross-section;
9. compute B_0 , α , B, P, and R for the breach channel using Eqs (16 - 19) (33 - 34);
10. compute sediment transport rate (Q_s) from Eq. (40);
11. compute ΔH_c as follows: $\Delta H_c = 3600 \Delta t \; Q_s / [P_0 L (1 - P_{or})]$ in which L is the length of the breach channel which may be easily computed from the geometric relations shown in Figure 2, P_{or} is the porosity of the breach material, and P_0 is the total perimeter of the breach, $P_0 = B_0 + 2 (H_u - H_c) / \cos \alpha$;
12. compute ΔH_c with the estimated value $\Delta H_c'$: if $100 (\Delta H_c' - \Delta H_c) / \Delta H_c < E$, where E is an error tolerance in percent (an input to the model having a value between 0.1 and 1.0), then the solution for ΔH_c and the associated outflows Q_b , Q_s, and Q_0 are considered acceptable; if the above inequality is not satisfied, step (2) is returned to with the recently

computed ΔH_e replacing $\Delta H_e'$; this cycle is repeated until convergence is attained, usually within 1 or 2 iterations.

13. check for collapse;
14. extrapolate estimates for $\Delta H_e'$ and $\Delta H'$;
15. if t is less than the specified duration of the computation (t_e) return to step 1 ; and
16. plot the outflow hydrograph consisting of the total flow ($Q_b + Q_s + Q_0$) computed at each time step.

Computational Requirements

The basic time step (Δt) is specified; however, when rapid erosion takes place the basic time step is automatically reduced to $\Delta t/20$. The specified value for the basic time step is usually about 0.02 hrs with slightly larger values acceptable for landslide dams. For typical applications, the BREACH model requires less than 10 seconds of CPU time on a Prime 750 computer and less than 2 seconds on an IBM 360/195 computer, both of which are main-frame quite amenable to such applications.

The model has displayed a lack of numerical instability or convergence problems. The computations show very little sensitivity to a reasonable variation in basic time step size. Numerical experimentation indicates that time of peak (T_p) , and final breach dimensions vary by less than 10, 4, and 0.5 percent, respectively.

Comparison with Previous Models

The BREACH model differs from the models of Cristofano (1965) and Harris and Wagner (1967) in the following significant ways:

1) the sediment transport algorithm utilized;
2) the method used for changing the breach shape and width;
3) the delay in breach erosion downward until the downstream face has been sufficiently eroded;
4) the introduction of a possible collapse mechanism for breach enlargement;
5) the accommodation of a piping failure mode; and
6) the consideration of possible tailwater submergence effects on the breach flow.

Similarities are their simplicity of the computational algorithm, the use of the D_{50} grain size and internal friction angle (ϕ) and the assumption of quasi-steady uniform flow hydraulics.

The BREACH model differs from the model reported by Ponce and Tsivoglou (1981) in the following significant ways:

1) items 1,2,4,5 and 6 as stated above;
2) the much simpler computational algorithm used in BREACH;
3) the use of the internal friction angle;
4) the use of the D_{50} grain size for determining the Manning n; and
5) consideration of spillway flows for man-made dams.

Similarities between the two models include the gradual development of the breach channel along the downstream face of the dam prior to its erosion vertically through the dam's crest, the use of the Manning n for the breach channel hydraulics, and the way in which the reservoir hydraulics are included in the development of the breach.

El documento original no contiene las páginas 86.

Appendix D

FAILURE DUE TO OVERTOPPING - CALCULATIONS

```
*****************************************************************************
*                                    * (program) S/N: 10132300              *
*                BREACH              * HMVersion    :  3.20                 *
*                                    * Date         : 12/03/93              *
*       Breach-Erosion Model         * Time         : 16:07:59              *
*   Hydrologic Research Laboratory   * Input file   : 04.dat                *
*                                    * Output file  : 04.out                 *
*                                    *                                       *
*                                    *                                       *
*****************************************************************************
```

```
xxxxxx   xxxxxx   xxxxxxx     xxx      xxxxx   x      x
x     x  x     x  x          x   x    x     x  x      x
x     x  x     x  x         x     x   x        x      x
xxxxxx   xxxxxx   xxxxx     xxxxxxx   x        xxxxxxx
x     x  x   x    x         x     x   x        x      x
x     x  x    x   x         x     x   x     x  x      x
xxxxxx   x     x  xxxxxxx   x     x    xxxxx   x      x
```

```
::::::::::::::::::::::::::::::::::::::::::::::
::::::::::::::::::::::::::::::::::::::::::::::
:::                                        :::
:::  Full Microcomputer Implementation    :::
:::                 by                     :::
:::        Haestad Methods, Inc.           :::
:::                                        :::
::::::::::::::::::::::::::::::::::::::::::::::
::::::::::::::::::::::::::::::::::::::::::::::
```

37 Brookside Road * Waterbury, Connecticut 06708 * (203) 755-1666

INPUT FILE:

```
 Kulekhani dam - data from KDPP.

HI=   5035.00 HU=   5032.74 HL=   4681.70 HPI=       .00 HSP=      .00 PI=  10.0 CA= .020 CB= .84

       (QIN(I),I=1,8)
     .00       .00       .00       .00       .00       .00       .00       .00

       (TIN(I),I=1,8)
     .00     40.00       .00       .00       .00       .00       .00       .00

       (RSA(I),I=1,8)
  539.30    467.63    381.62    294.12    132.73     42.51      4.20       .00

       (HSA(I),I=1,8)
 5019.62   4986.81   4954.00   4921.20   4822.77   4757.16   4691.54   4681.70

       (HSTW(I),I=1,8)
 4681.70   5032.74       .00       .00       .00       .00       .00       .00

       (BSTW(I),I=1,8)
     .00   1500.00       .00       .00       .00       .00       .00       .00

       (QMTW(I),I=1,8)
     .03       .03       .00       .00       .00       .00       .00       .00

ZU=  2.00 ZD=  1.80 ZC=   .50 GL=   .00 GS=   .00 VMP=   .00

D50C=  1.00 PORC=   .39 UWC=124.00 CNC=1.0000 AFRC= 30.00 COHC= 941.0 UNFCC=100.00

D50S=  5.00 PORS=   .29 UWS=120.00 CNS=1.0000 AFRS=  2.37 COHS=    .0 UNFCS= 12.00

BR=  2.00 WC=  30.0 CRL= 1302.0 SM=150.00 D50DF=   .00 UNFCDF=   .00 BMX=    0.

DTH=  .050 DBG=  .000 H=   .1000 TEH=   40.0 ERR=   .01 FPT=   2.0 TPR=    .0
```

- o - 0 - o -

OUTPUT SUMMARY

QBP	MAX OUTFLOW(CFS) THRU BREACH	99859.
TP	TIME(HR) AT WHICH PEAK OUTFLOW OCCURS	2.10
QP	MAX TOTAL OUTFLOW(CFS) OCCURRING AT TIME TP	99859.
TRS	DURATION(HR) OF RISING LIMB OF HYDROGRAPH	2.05
TB	TIME(HR) AT WHICH SIGN. RISE IN OUTFLOW STARTS	.05
BRD	FINAL DEPTH(FT) OF BREACH	351.04
BRW	FINAL TOP WIDTH(FT) OF BREACH AT PEAK BREACH FLOW	10.07
HU	ELEV(FT) OF TOP OF DAM	5032.74
HY	FINAL ELEV(FT) OF RESERVOIR WATER SURFACE	4742.19
HC	FINAL ELEV(FT) OF BOTTOM OF BREACH	4681.700
AGL	ACUTE ANGLE THAT BREACH SIDE MAKES WITH VERTICAL AT QBP	2.289
QO	OUTFLOW (CFS) AT T=0.0	51.3635
Z	SIDE SLOPE OF BREACH (FT/FT) AT PEAK BREACH FLOW	.01
TFH	TIME OF FAILURE (HR) WHICH IS LINEAR EQUIVALENT OF TRS OBTAINED BY USING SIMPLIFIED DAM-BREAK DISCHARGE EQUATION	15.55
TFHI	TIME OF FAILURE (HR) WHICH IS LINEAR EQUIVALENT OF TRS OBTAINED BY INTEGRATING QB VS TIME FROM T=0 TO T=TP	1.69
BO	BOTTOM WIDTH (FT) OF BREACH AT PEAK BREACH FLOW	5.21

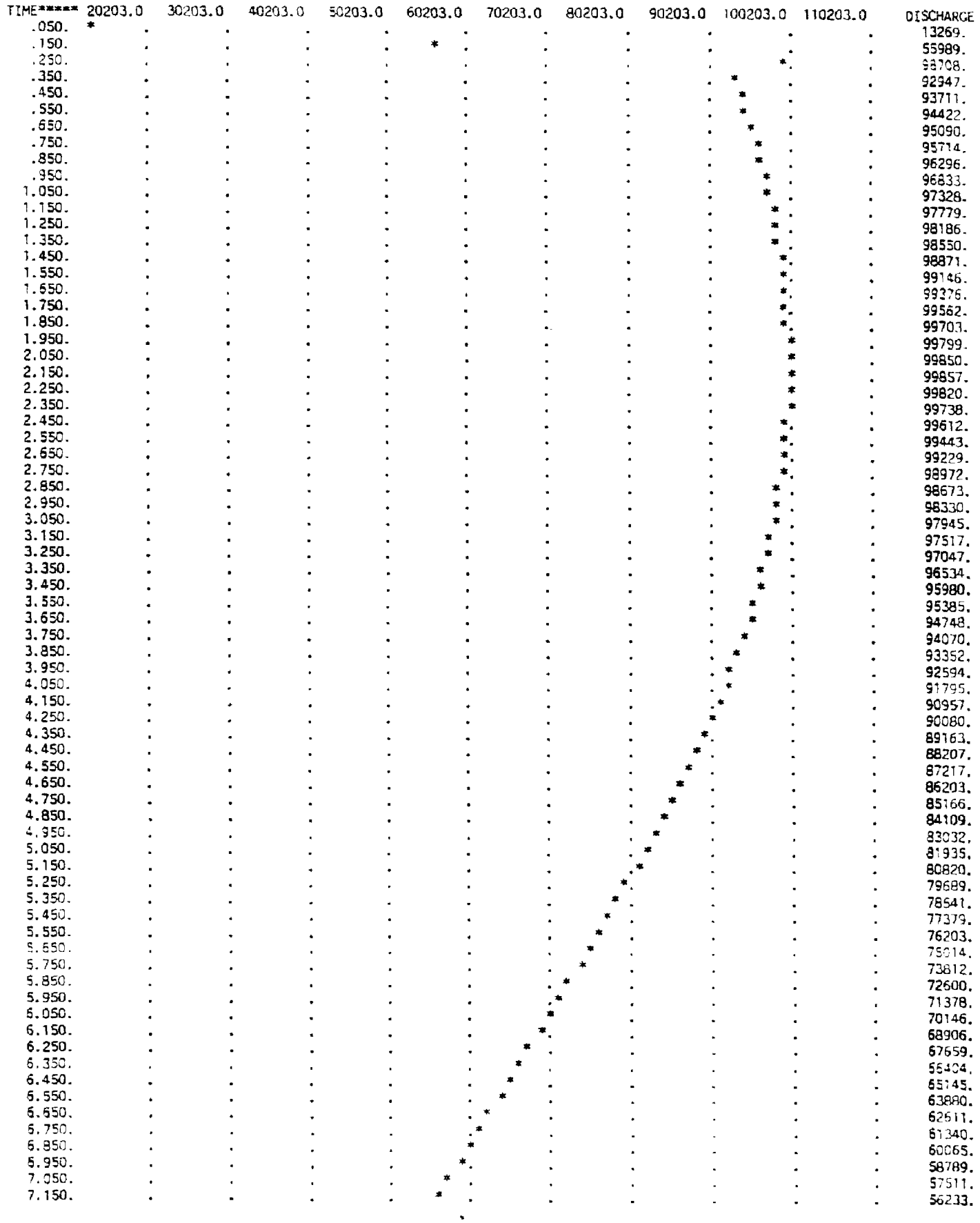
TIME*****
20203.0
30203.0
40203.0
50203.0
60203.0
70203.0
80203.0
90203.0
100203.0
110203.0
DISCHARGE
.050. 13269.
.150. 55989.
.250. 88708.
.350. 92947.
.450. 93711.
.550. 94422.
.650. 95090.
.750. 95714.
.850. 96296.
.950. 96833.
1.050. 97328.
1.150. 97779.
1.250. 98186.
1.350. 98550.
1.450. 98871.
1.550. 99146.
1.650. 99376.
1.750. 99562.
1.850. 99703.
1.950. 99799.
2.050. 99850.
2.150. 99857.
2.250. 99820.
2.350. 99738.
2.450. 99612.
2.550. 99443.
2.650. 99229.
2.750. 98972.
2.850. 98673.
2.950. 98330.
3.050. 97945.
3.150. 97517.
3.250. 97047.
3.350. 96534.
3.450. 95980.
3.550. 95385.
3.650. 94748.
3.750. 94070.
3.850. 93352.
3.950. 92594.
4.050. 91795.
4.150. 90957.
4.250. 90080.
4.350. 89163.
4.450. 88207.
4.550. 87217.
4.650. 86203.
4.750. 85166.
4.850. 84109.
4.950. 83032.
5.050. 81935.
5.150. 80820.
5.250. 79689.
5.350. 78541.
5.450. 77379.
5.550. 76203.
5.650. 75014.
5.750. 73812.
5.850. 72600.
5.950. 71378.
6.050. 70146.
6.150. 68906.
6.250. 67659.
6.350. 66404.
6.450. 65145.
6.550. 63880.
6.650. 62611.
6.750. 61340.
6.850. 60065.
6.950. 58789.
7.050. 57511.
7.150. 56233.

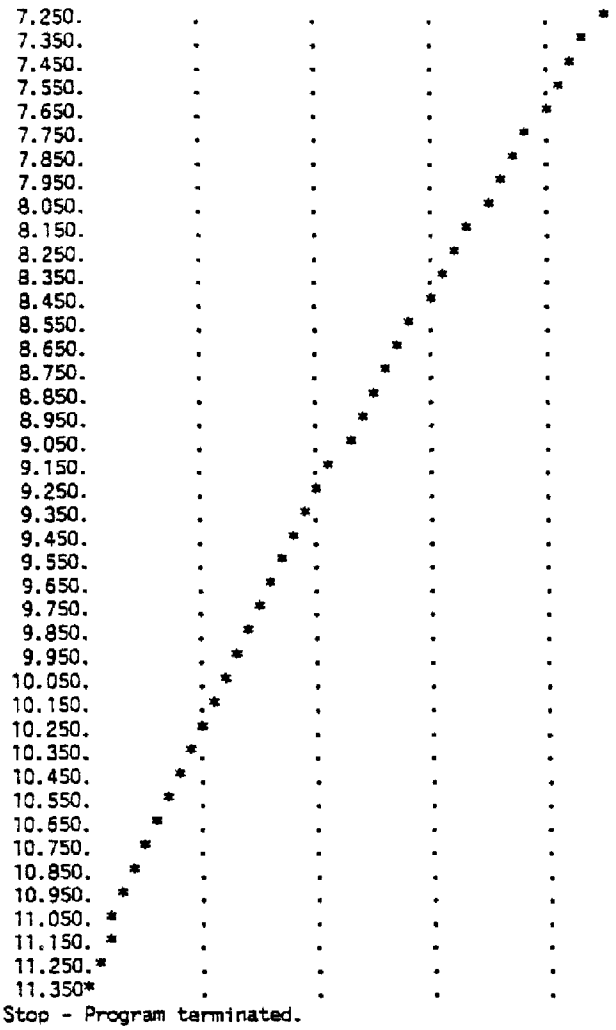

7.250.	54955.
7.350.	53678.
7.450.	52402.
7.550.	51128.
7.650.	49856.
7.750.	48588.
7.850.	47323.
7.950.	46062.
8.050.	44805.
8.150.	43552.
8.250.	42305.
8.350.	41063.
8.450.	39831.
8.550.	38613.
8.650.	37408.
8.750.	36217.
8.850.	35040.
8.950.	33877.
9.050.	32728.
9.150.	31594.
9.250.	30474.
9.350.	29368.
9.450.	28277.
9.550.	27200.
9.650.	26138.
9.750.	25089.
9.850.	24054.
9.950.	23033.
10.050.	22024.
10.150.	21028.
10.250.	20043.
10.350.	19069.
10.450.	18105.
10.550.	17149.
10.650.	16200.
10.750.	15255.
10.850.	14312.
10.950.	13396.
11.050.	12530.
11.150.	11710.
11.250.*	10936.
11.350*	10204.

Stop - Program terminated.

Appendix E

FAILURE DUE TO PIPING - CALCULATIONS

```
*****************************************************************************
*                                 * (program) S/N: 10132300                 *
*            BREACH               * HMVersion    :  3.20                    *
*                                 * Date         : 12/03/93                 *
*      Breach-Erosion Model       * Time         : 14:47:32                 *
*  Hydrologic Research Laboratory * Input file   : p-01.dat                 *
*                                 * Output file  : p-01.out                 *
*                                 *                                         *
*                                 *                                         *
*****************************************************************************
```

```
xxxxxx   xxxxxx   xxxxxxx    xxx     xxxxx   x     x
x     x  x     x  x          x   x   x     x  x     x
x     x  x     x  x         x     x  x        x     x
xxxxxx   xxxxxx   xxxxx     xxxxxxx  x        xxxxxxx
x     x  x   x    x         x     x  x        x     x
x     x  x    x   x         x     x  x     x  x     x
xxxxxx   x     x  xxxxxxx  x     x   xxxxx   x     x
```

```
::::::::::::::::::::::::::::::::::::::::::::::
::::::::::::::::::::::::::::::::::::::::::::::
:::                                        :::
:::  Full Microcomputer Implementation    :::
:::                  by                    :::
:::        Haestad Methods, Inc.           :::
:::                                        :::
::::::::::::::::::::::::::::::::::::::::::::::
::::::::::::::::::::::::::::::::::::::::::::::
```

37 Brookside Road * Waterbury, Connecticut 06708 * (203) 755-1666

INPUT FILE:

```
Kulekhani dam - data from KDPP - PIPING FAILURE.

HI=  5035.00 HU=  5032.74 HL=  4681.70 HPI=  4700.00 HSP=     .00 PI= 10.0 CA= .020 CB= .84

      (QIN(I),I=1,8)
    .00      .00      .00      .00      .00      .00      .00      .00

      (TIN(I),I=1,8)
    .00    40.00      .00      .00      .00      .00      .00      .00

      (RSA(I),I=1,8)
 539.30   467.63   381.62   294.12   132.73    42.51     4.20      .00

      (HSA(I),I=1,8)
5019.62  4986.81  4954.00  4921.20  4822.77  4757.16  4691.54  4681.70

      (HSTW(I),I=1,8)
4681.70  4690.00  4700.00  4710.00  4720.00  5000.00      .00      .00

      (BSTW(I),I=1,8)
    .00    10.00    20.00    30.00    40.00   320.00      .00      .00

      (CMTW(I),I=1,8)
    .03      .03      .03      .03      .03      .03      .00      .00

ZU= 2.00 ZD= 1.80 ZC=  .50 GL=  .00 GS=  .00 VMP=  .00

D50C= 1.00 PORC=  .01 UWC=124.00 CNC=1.0000 AFRC= 30.00 COHC= 941.0 UNFCC=100.00

D50S= 5.00 PORS=  .29 UWS=120.00 CNS=1.0000 AFRS= 2.37 COHS=   .0 UNFCS= 12.00

BR= 1.00 WC= 30.0 CRL= 1302.0 SM=150.00 D50DF=  .00 UNFCDF=  .00 BMX=   0.

DTH= .050 DBG= .000 H=  .1000 TEH=  40.0 ERR=  .01 FPT=  1.0 TPR=   .0
```

- o - 0 - o -

OUTPUT SUMMARY

QBP	MAX OUTFLOW(CFS) THRU BREACH	1399140.
TP	TIME(HR) AT WHICH PEAK OUTFLOW OCCURS	.56
QP	MAX TOTAL OUTFLOW(CFS) OCCURRING AT TIME TP	1399140.
TRS	DURATION(HR) OF RISING LIMB OF HYDROGRAPH	.41
TB	TIME(HR) AT WHICH SIGN. RISE IN OUTFLOW STARTS	.00
BRD	FINAL DEPTH(FT) OF BREACH	351.04
BRW	FINAL TOP WIDTH(FT) OF BREACH AT PEAK BREACH FLOW	128.18
HU	ELEV(FT) OF TOP OF DAM	5032.74
HY	FINAL ELEV(FT) OF RESERVOIR WATER SURFACE	4809.44
HC	FINAL ELEV(FT) OF BOTTOM OF BREACH	4681.700
AGL	ACUTE ANGLE THAT BREACH SIDE MAKES WITH VERTICAL AT QBP	.117
QO	OUTFLOW (CFS) AT T=0.0	.0875
Z	SIDE SLOPE OF BREACH (FT/FT) AT PEAK BREACH FLOW	.00
TFH	TIME OF FAILURE (HR) WHICH IS LINEAR EQUIVALENT OF TRS OBTAINED BY USING SIMPLIFIED DAM-BREAK DISCHARGE EQUATION	1.33
TFHI	TIME OF FAILURE (HR) WHICH IS LINEAR EQUIVALENT OF TRS OBTAINED BY INTEGRATING QB VS TIME FROM T=0 TO T=TP	.56
BO	BOTTOM WIDTH (FT) OF BREACH AT PEAK BREACH FLOW	128.18

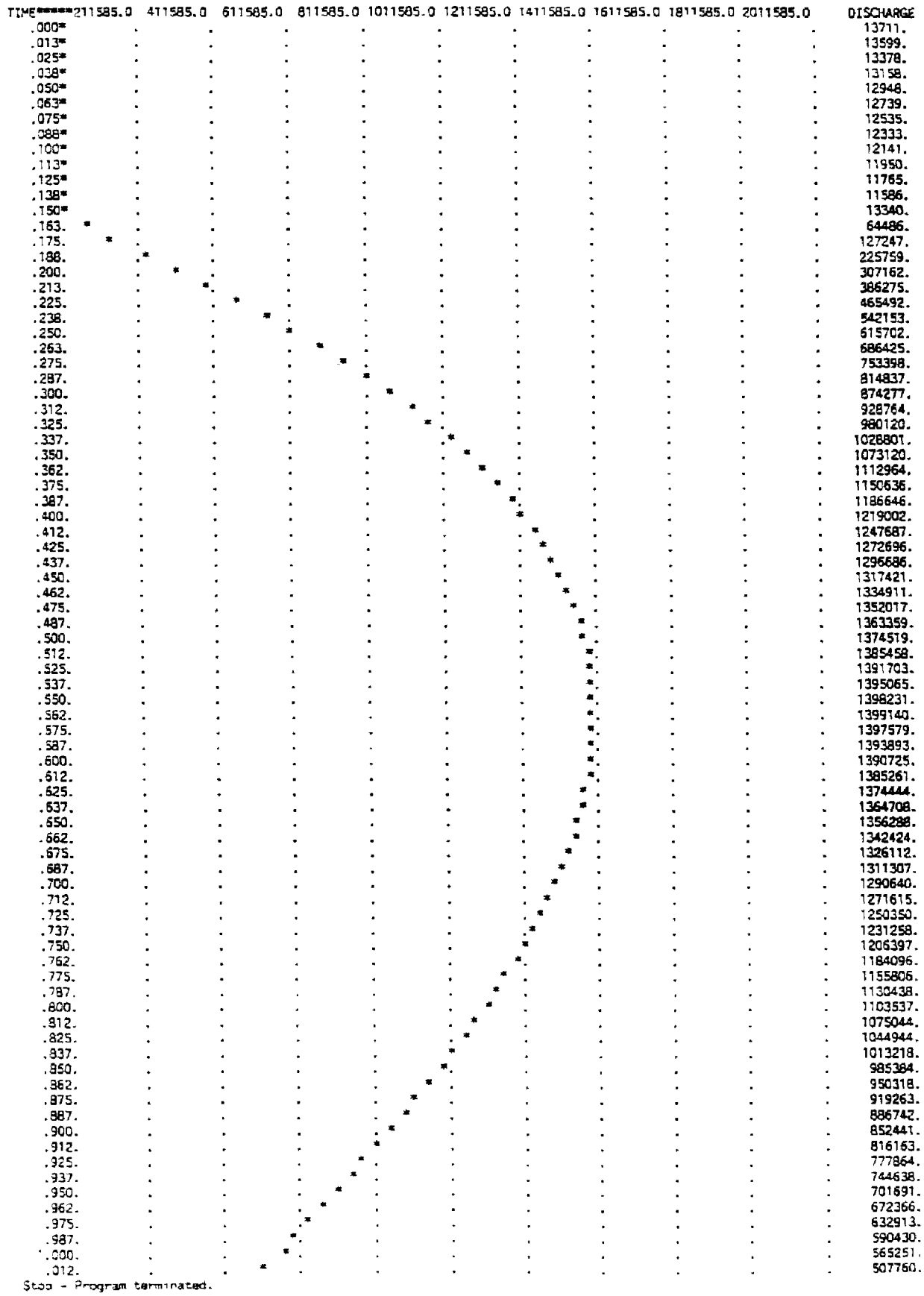
TIME*****211585.0 411585.0 611585.0 811585.0 1011585.0 1211585.0 1411585.0 1611585.0 1811585.0 2011585.0 DISCHARGE
.000* 13711.
.013* 13599.
.025* 13378.
.038* 13158.
.050* 12948.
.063* 12739.
.075* 12535.
.088* 12333.
.100* 12141.
.113* 11950.
.125* 11765.
.138* 11586.
.150* 13340.
.163. 64486.
.175. 127247.
.188. 225759.
.200. 307162.
.213. 386275.
.225. 465492.
.238. 542153.
.250. 615702.
.263. 686425.
.275. 753398.
.287. 814837.
.300. 874277.
.312. 928764.
.325. 980120.
.337. 1028801.
.350. 1073120.
.362. 1112964.
.375. 1150636.
.387. 1186646.
.400. 1219002.
.412. 1247687.
.425. 1272696.
.437. 1296686.
.450. 1317421.
.462. 1334911.
.475. 1352017.
.487. 1363359.
.500. 1374519.
.512. 1385458.
.525. 1391703.
.537. 1395065.
.550. 1398231.
.562. 1399140.
.575. 1397579.
.587. 1393893.
.600. 1390725.
.612. 1385261.
.625. 1374444.
.637. 1364708.
.650. 1356288.
.662. 1342424.
.675. 1326112.
.687. 1311307.
.700. 1290640.
.712. 1271615.
.725. 1250350.
.737. 1231258.
.750. 1206397.
.762. 1184096.
.775. 1155806.
.787. 1130438.
.800. 1103537.
.812. 1075044.
.825. 1044944.
.837. 1013218.
.850. 985384.
.862. 950318.
.875. 919263.
.887. 886742.
.900. 852441.
.912. 816163.
.925. 777864.
.937. 744638.
.950. 701691.
.962. 672366.
.975. 632913.
.987. 590430.
1.000. 565251.
.012. 507760.
Stop - Program terminated.